International Journal of Engineering Research and Science & Technology

IJERST

www.ijerst.org

ISSN : 2319-5991

Vol. 21 No. 3 (1) 2025

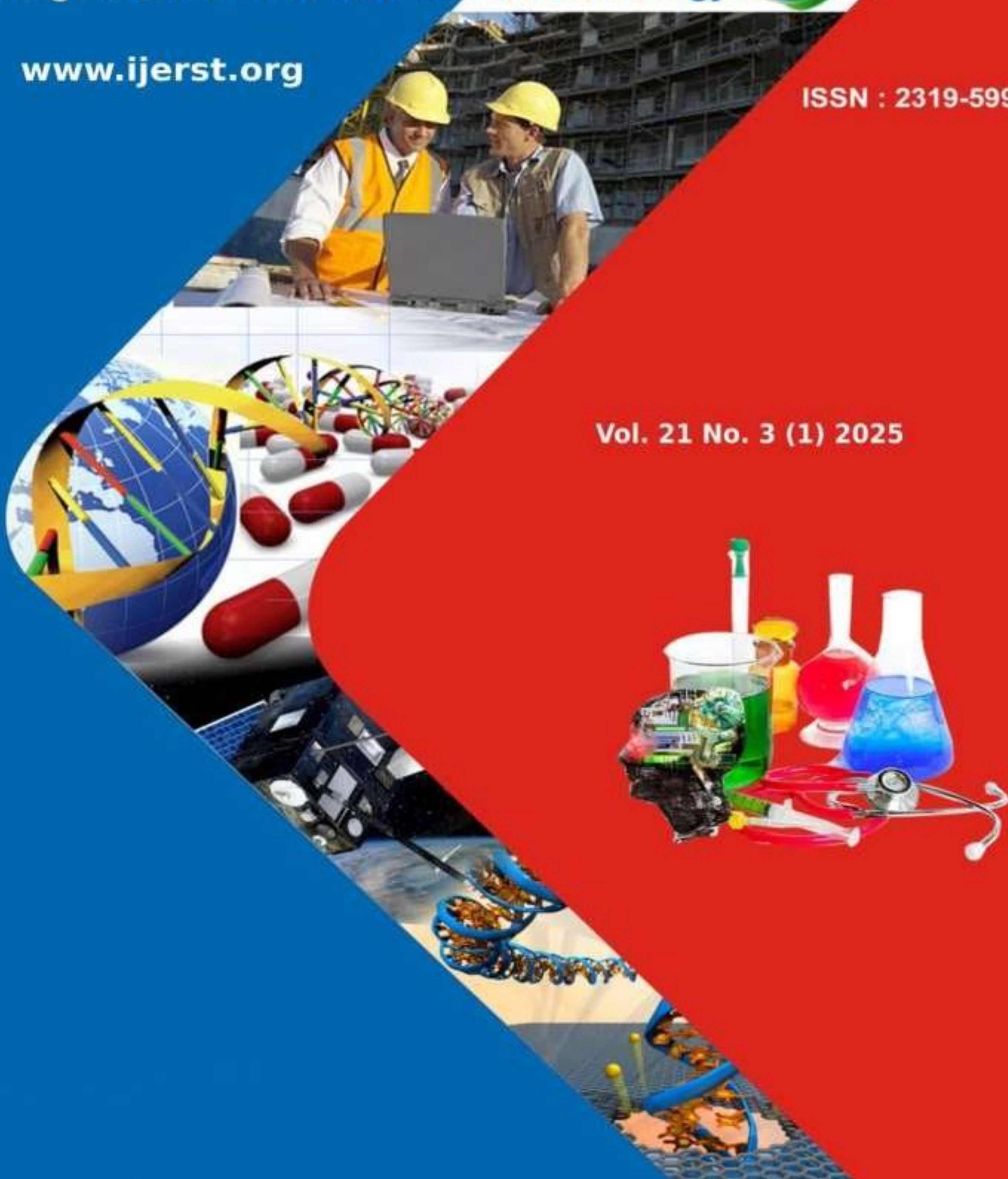

ijerst.editor@gmail.com

editor@ijerst.com

FUZZY LOGIC-BASED VSG-CONTROLLED DUAL-STAGE PV-BATTERY SYSTEM

Gundeti Meghana[1], Dr. V. Satyanarayana[2]

[1]M. Tech Student, Department of Electrical and Electronics Engineering, Vaagdevi College of Engineering, Khammam - Warangal Hwy, Road, Bollikunta, Telangana 506005

[2]Associate Professor, Department of Electrical and Electronics Engineering, Vaagdevi College of Engineering, Khammam - Warangal Hwy, Road, Bollikunta, Telangana 506005

Abstract *This study uses a Virtual Synchronous Generator (VSG) control method to present a fuzzy logic-based control system for a two-stage converter in a freestanding PV battery system. The standalone setup seeks to provide energy stability and dependability for off-grid applications by combining a photovoltaic (PV) array with a battery energy storage system (BESS). By offering virtual inertia and damping, the VSG technique allows the system to replicate the behaviour of traditional synchronous generators, improving the standalone microgrid's stability during variations in load and generation. A two-stage converter makes up the system; the first stage uses a Maximum Power Point Tracking (MPPT) algorithm to maximize PV power output, while the second stage uses the BESS to control voltage regulation and power delivery. Based on real-time system variables, such as load demands and variations in solar irradiation, a fuzzy logic controller is used to adaptively modify VSG parameters, such as virtual inertia and damping coefficients. This method increases the standalone microgrid's dynamic reactivity and improves the system's resistance to brief disruptions. The usefulness of the suggested fuzzy logic-based VSG control system is confirmed by simulation results, which show enhanced frequency and voltage stability, effective power management, and smooth load-sharing between the battery and the PV array. The research emphasises how sophisticated control systems may help develop off-grid and distant independent renewable energy solutions.*

Keywords: *Photovoltaic, Virtual synchronous generator, MATLAB, MPPT, Fuzzy logic controller*

Received: 29-07-2025 Accepted: 20-08-2025 Published: 29-08-2025

1. INTRODUCTION

The predominant interest in photovoltaic structures among distributed turbines is attributed to their simplicity of installation and long-term sustainability. The cost of solar panels has significantly decreased, yet they often provide inconsistent DC power. Prior to connecting the PV indicators to the grid or supplying them to the output load, they must first be converted from DC to AC or DC to DC. Unreliable photovoltaic power requires an electrical storage device, often a battery bank, for independent photovoltaic systems. Over time, photovoltaic (PV) delivery fluctuates owing to the inherent variability of the supply and the conditions dictated by the load or grid specifications. Multiple methods exist to integrate solar energy into the grid or load.

Initially, inverters may be used to convert DC power into AC voltage according to the load's requirements. The two-dimensional option entails enhancing the direct current voltage supplied by photovoltaic cells and then converting it to alternating current as necessary. Recent interest in the designs of stage grid converters for use in isolation has been little among the scholarly community. We developed an independent, two-degree, single-segment photovoltaic machine.

The scientists concluded that the system could enough generate power autonomously, negating the need for batteries. Consequently, the upkeep and spending ramifications will be less for a system that is constructed more practically. This work presented a two-stage independent system control architecture based on a proportional integral (PI) method. The findings indicated that the control objectives were achieved well. A two-stage converter employs VSG control, although the previously stated papers do not elucidate its operation. This article focused on an autonomous two-stage converter powered by batteries, specifically in relation to the VSG control system application.

2. MATHEMATICAL MODELLING

Solar cell modeling

The circuit analogous to a photovoltaic cell is shown below. A contemporary power supply and a diode are connected in parallel to manage the solar mobile.

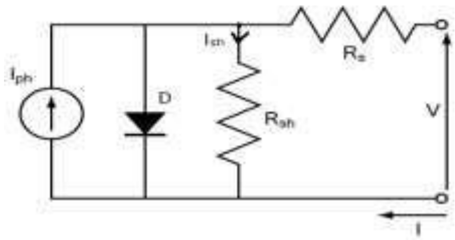

FIGURE 1 Solar PV module equivalent circuit

For the above circuit, apply KCL (Kirchoff's Current Law) we have [1]

$$I_{ph} = I_d + I_{sh} + I$$

$$I = I_{ph} - (I_{sh} + I)$$

We have the following equation for the Solar cell current

$$I = I_{ph} - (I[e\ (V + I.R_s)/V_T) - 1] - (V + R_s)/R_{sh}$$

Where I_{ph} denotes isolation modern-day

I symbolise cellular forex.

Io represents the inverse saturation modern-day

V denotes the cellular voltage.

Rs signifies Series Resistance:

Rsh denotes Shunt Resistance.

V_T denotes Terminal Voltage

DESIGN OF THE CONVERTER DC-DC

The continuous use of DC-to-DC converters with photovoltaic modules optimises overall performance and maximises energy efficiency. This is achieved by the use of converters such as dollar, raise, and greenback-enhance. Battery charging programs use a buck-boost mechanism, whereas grid-connected systems utilise a boost converter. The constituents of a boost converter are a DC input voltage source Vs, a load resistance R, a smoothing capacitor C, a diode D, a control switch S, and an inductive element L. The figure illustrates the configuration of such components. The voltage gains of the rise converter may be articulated by assuming a duty cycle ratio D for the transfer.

$$M_v = V_o/V_s = 1/1 - D$$

The pulse width modulation (PWM) signal is used to alter the ON and OFF states of MOSFETs; the variables V_o, V_s, and D represent the input voltage, output voltage, and duty cycle, respectively.

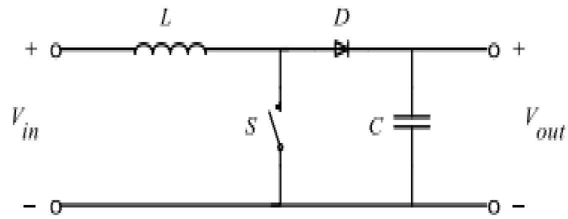

FIGURE 2 Circuit diagram for the boost converter

A improve converter is used to get the preferred voltage. The body structural structure for the DC-DC degree is shown in Figure 2. The definitions of the layout necessities are as follows:

Vin = one hundred–a hundred and fifty V, fsw = 5 kHz, and Vout = 500 Vdc are the input voltage and switching frequency, respectively. The specifications kingdom that the rated electricity is 5 kW, the modern ripple is 5%, and the voltage ripple is 1%. Iin is between 33 and 50 A, while ΔI is among 1.65 and a couple of.5.

The inductance capacitance is calculated as:

$$L = \frac{V_{in}(V_{out} - V_{in})}{fsw^{*}\Delta I^{*}V_{out}} = 6.4 \text{ to } 12.7\text{mH}$$

$$C = \frac{I_{out}(V_{out} - V_{in})}{fsw^{*}\Delta V^{*}V_{out}} = 280 \text{ to } 320\mu\text{F}$$

3. PROPOSED SYSTEM

Figure: Presents a design for a level converter. Connected to the PV power source via a bidirectional converter, one may see DC-DC, DC-AC, and garage units that resource electricity to the load. The device also includes the control systems for the two levels.

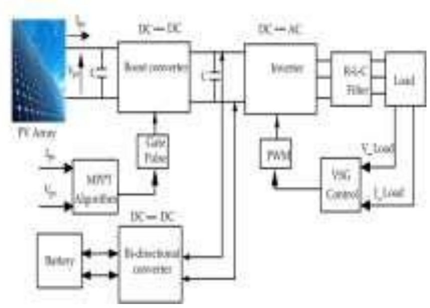

FIGURE 3 Schematic circuit diagram for a two-stage converter

CONTROL STRATAGY

MPPT ALGORITHM CONTROL

The method for figuring out the sun unit's most power output the use of the obligation-cycle controlled float chart MPPT technique is proven in the block diagram that follows. The photovoltaic system's voltage and contemporary decide the solar panel's specs. In the duty-cycle manipulate method, the voltage of america energy is calculated by multiplying the modern-day and voltage from the sun panels through the preceding variety. Likewise, based at the associated strength output, it guarantees adherence to the most pressure requirement and compares the cost of voltage sampling to the preceding fee.

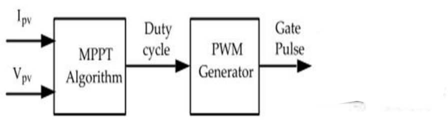

FIGURE 4 MPPT I/O block diagram

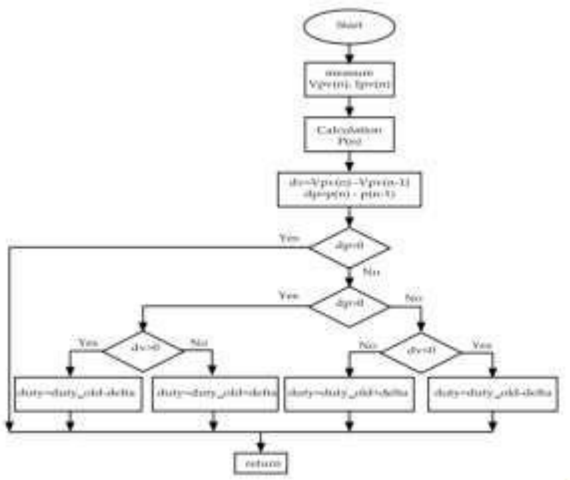

FIGURE 5 Duty cycle control algorithm

VSG METHOD

The control circuit and strength load make up an inverter's block diagram in a VSG-primarily based system (Fig.). This stage takes the burden's cutting-edge and voltage as enter and produces the pulse width modulation (PWM) signal that controls the inverter.

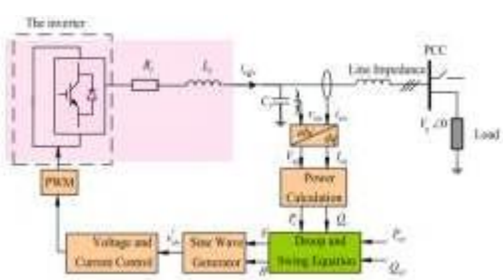

FIGURE 6 Structure of VSG control

The VSG active and reactive power loops are described in below figures respectively.

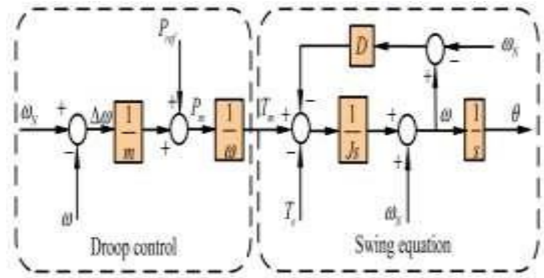

FIGURE 7 The active power loop of VSG

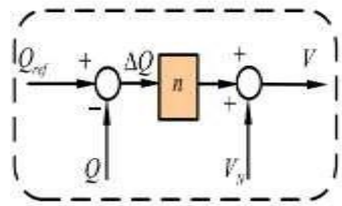

FIGURE 8 The reactive power-voltage droop control loop of VSG

The droop equations are expressed as:

$$\omega = \omega_N - m(P - P_{ref})$$
$$V = V_N - n(Q - Q_{ref})$$

The swing equations are expressed as

$$J\omega\frac{d(\omega-\omega_N)}{dt} = P_{ref} - P_e - D(\omega-\omega_N) + \frac{1}{m}(\omega_N - \omega)$$

Charge–discharge battery controller

The illustration shows that the battery control works properly while the battery is charged or discharged. The bidirectional converter receives voltage from the upgraded converter. The specs of the battery are shown in Table 1. Battery current is denoted by the letter IB, while battery voltage is denoted by the symbol VB. We have the IB-ref rate as the reference rate. Cha., and we have IB-ref for today's discharge. Dis. There is a positive pulse (S-P) and a negative pulse (S-N) in the bidirectional converter.

Table 1: The battery parameters

Quantity	Value
Nominal voltage	220 V
Rated capacity (Ah)	100
Initial SOC %	50
Fully charged voltage	256 V

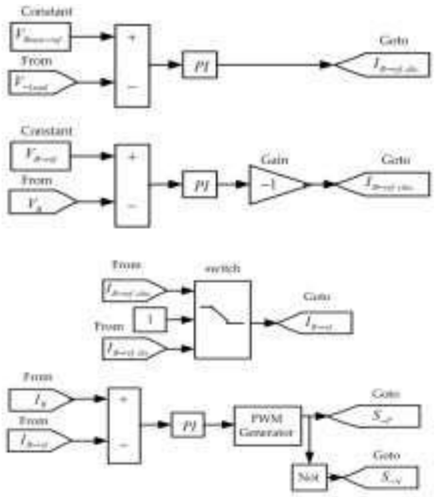

FIGURE 9 MATLAB simulation battery charge and discharge control

4. FUZZY LOGIC CONTROL

Fuzzy common sense may be defined in several ways. In its narrowest meaning, fuzzy common sense is a system of reasoning that expands upon multivalve common sense. In a larger sense, fuzzy common sense (FL) is quite similar to fuzzy set principle. In fuzzy logic, a fuzzy unit is a device instruction with a degree-dependent club that lacks sharp edges. Fuzzy good judgement is a subset of fuzzy logic (fl) in this context. Even when its scope is reduced, fuzzy logic remains conceptually and substantively particular in comparison to traditional multivalve logical systems. Think about fuzzy good judgement (FL) or fuzzy common sense (in its widest sense) to maximise your use of fuzzy Logic Toolbox. The fundamental ideas of fuzzy logic are laid forth in a clear and succinct manner in Foundations of Fuzzy Logic. Also, keep in mind that the primary concept of a linguistic variable—one whose values are words instead of numbers—is central to FL. Essentially, FL might be seen as a method of calculating using words instead of numbers. While they aren't as precise as statistics, they are more in accordance with human intuition. The response cost is decreased since computing with phrases also makes advantage of the tolerance for imprecision.

Prioritising the utility of a roughly expected response above the expense of precision is fundamental to fuzzy logic. The Fuzzy Logic Toolbox is an effective tool for dealing with issues related to fuzzy good judgement when used with the technical laptop application MATLAB. Fuzzy common sense research is fascinating because it attempts to model the age-old human skill of weighing importance and correctness. While fuzzy logic as a field of cutting-edge science is relatively new, the idea behind it is founded on tried-and-true human reasoning abilities, thus fuzzy common sense is, in a way, both new and old.

5. SIMULATION RESULTS

Existing system results

A. SCENARIO A: DIFFERENT IRRADIANCE VALUES

The Fig.10 shows the MATLAB/SIMULINK circuit diagram of the system in Scenario A and the Fig.10.1 shows the irradiation applied to the PV. The curve, as shown in the figure, contains various irradiations with a maximum value of 1000 W\m^{2}. The PV voltage and first stage voltage followed the change in radiation, as shown in Fig.10.2 (i) and Fig.10.2 (ii) respectively. At the first stage, the PV rise to 130 Volts and boosted voltage to 500 Volts. This is caused by the nature of the MPPT method in PV, and it provided details for the control behavior. The current results of the PV array and boost converter output are given in Fig.10.3 (i) and Fig.10.3 (ii), respectively. The PV current is approximately 50 A, while the boost converter current decreases to 10 A. This decrease depends on the design of the boost converter. Fig.10.4 shows the results of the inverter voltage and current for the output load. The inverter side is connected with the load and the output power waveforms shown in Fig. 10.5.

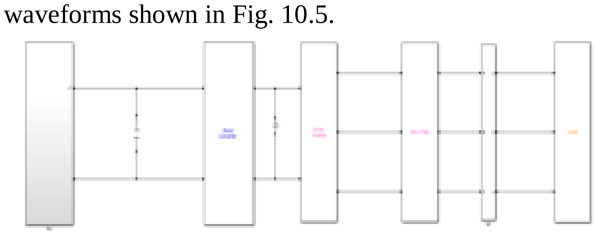

FIGURE 10 MATLAB/SIMULINK circuit diagram of the system in Scenario A

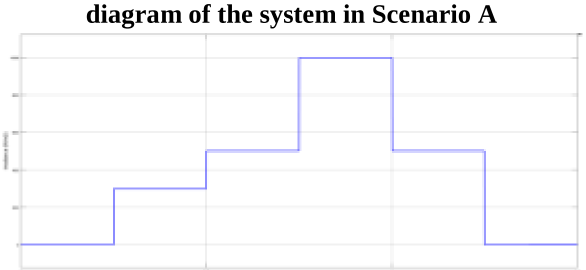

FIGURE 10.1 The irradiation scheme

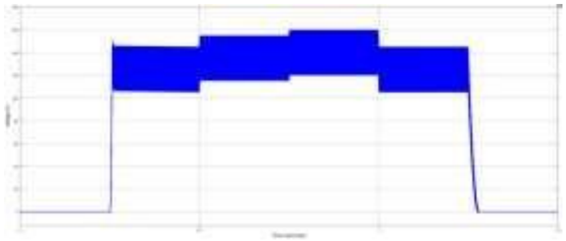

(i)

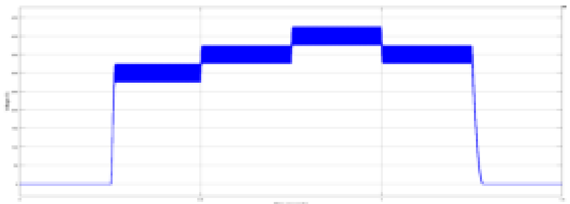

(ii)

FIGURE 10.2 Voltage results: (i) PV voltage; (ii) boost converter voltage

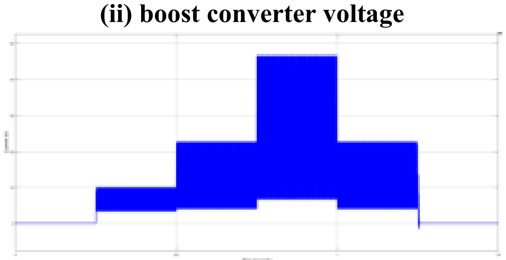

(i)

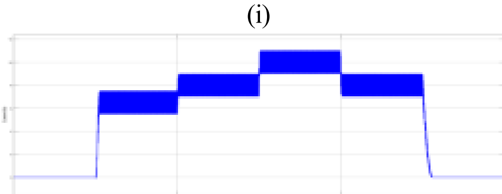

(ii)

FIGURE 10.3 Current waveforms: (i) PV current; (ii) boost converter output current

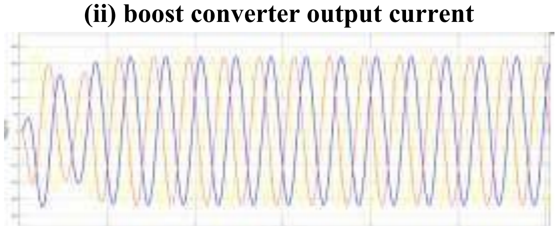

(i)

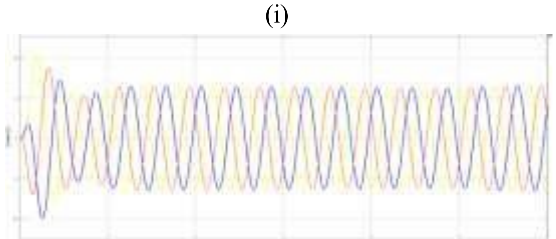

(ii)

FIGURE 10.4 The output load: (i) voltage; (ii) current

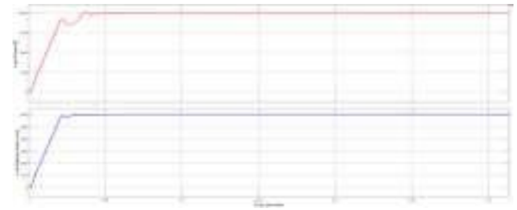

FIGURE 10.5 The load active and reactive power

B. SCENARIO B: IRRADIANCE CURVE VALUES

The MATLAB/SIMULINK circuit schematic of the machine in Scenario B and Fig.10.6 are suggested in Fig. 10.7. The irradiation applied to the PV is suggested by number eight.

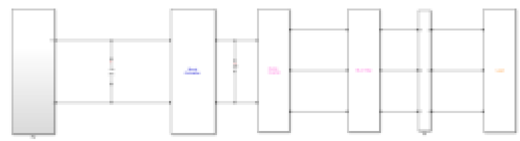

FIGURE 10.6 MATLAB/SIMULINK circuit diagram of the system in Scenario B

Several values for the curve are clearly shown by the determination. An updated irradiation curve depicted in Figure 10.8 depicts the voltage response between the PV voltage and the DC-DC converter output voltage. The VSG management approach was put into place as a result of the mission's higher performance output. The inverter can be used as a synchronous generator with this type of control. This makes it possible for multiple inverters to work together and makes it easier to store power in an especially vulnerable grid or islanding mode. The solar array and improved rise converter are shown in Fig 10.9. Fig.10.10 depicts the impact that the cutting edge and inverter voltage have on the output load. Fig.10.11 depicts the characteristics of the inverter as well as the load- related output energy waveforms.

FIGURE 10.7 The irradiation curve scheme

FIGURE 10.8 The PV and boost converter voltage

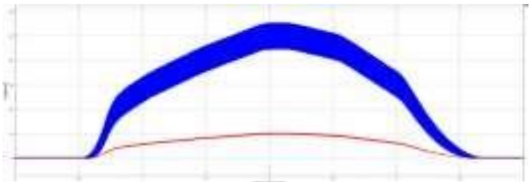

FIGURE 10.9 The PV and boost converter current

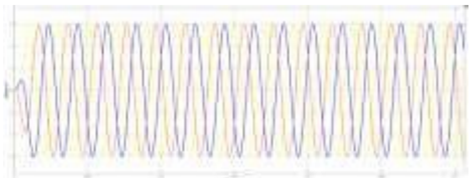

(i)

FIGURE 10.10 The output load: (i) voltage; (ii) current

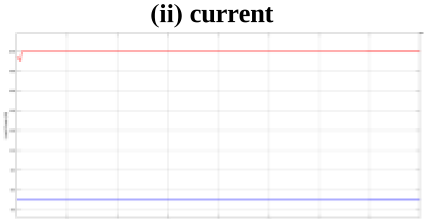

FIGURE 10.11 The load active and reactive power

C. SCENARIO C: BATTERY CHARGE AND DISCHARGE

The Fig 10.12 shows the MATLAB/SIMULINK circuit diagram of the system in Scenario B in charging mode. The arrangement as shown in below figure.

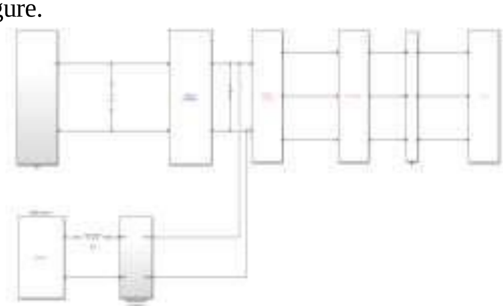

FIGURE 10.12 MATLAB/SIMULINK circuit diagram of the system in Scenario C (CHARGE MODE)

Both the charging and discharging situations use a bidirectional converter for batteries. The battery became capable of charging simultaneously with the load owing to the voltage deliverer's "boost converter output." A bidirectional converter is used when the battery requires charging or discharging. Upon the implementation of the load voltage, the voltage supply known as the "enhance converter output" facilitated the battery's elevation to 237.5 volts, as seen in Figures 10.13 (ii) and 10.13 (iv). The current charging rate for the battery in this mode is 10 A, whereas the reference charging current for the battery is 20 A, as seen in Figure 10.13 (iii).

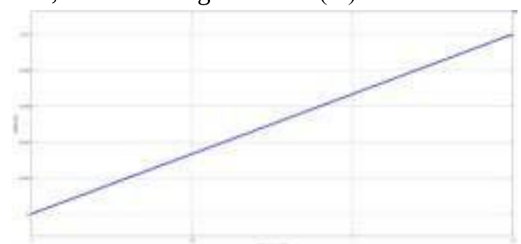

(i)

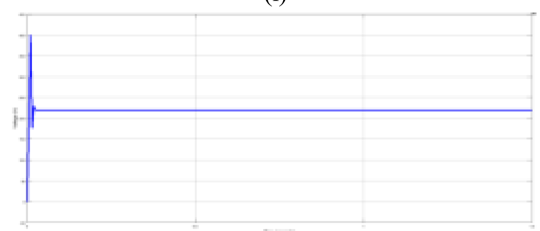

(ii)

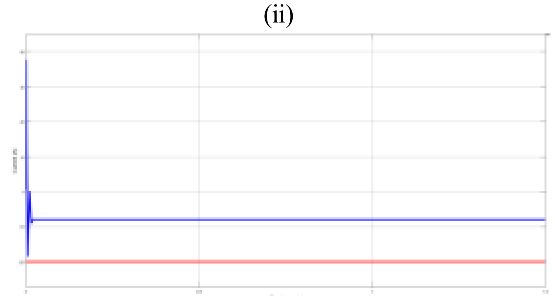

(iii)

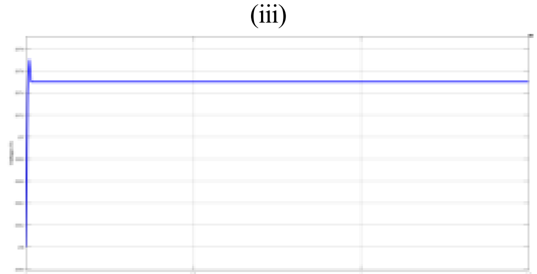

(iv)

FIGURE 10.13 Battery charge mode: (i) the state of charge; (ii) load voltage; (iii) reference and battery current; (iv) battery voltage

In discharge mode, the load is supplied by the battery, and the output voltage is disabled. The operation of discharge is shown in Fig.10.14. The battery is depleted at 236 V and 21 A, with the standard reference being 20 A. Scenarios A and B both include the connection of the battery. The battery performance in circumstances A and B is equal to that in scenario C.

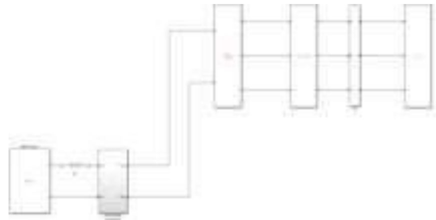

FIGURE 10.14 MATLAB/SIMULINK circuit diagram of the system in Scenario C (DISCHARGE MODE)

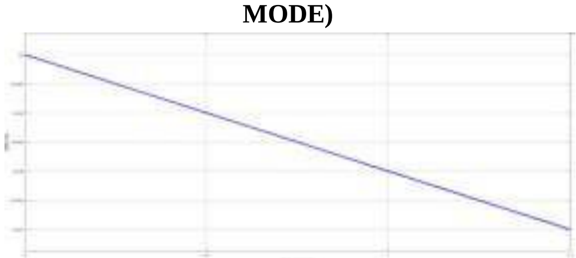

(i)

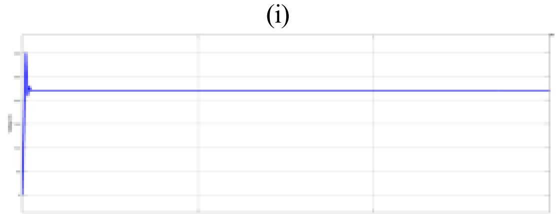

(ii)

(iii)

(iv)

FIGURE 10.15 Battery discharge mode: (i) the state of charge; (ii) load voltage; (iii) reference and battery current; (iv) battery voltage

D. SCENARIO D: THE BEHAVIOR OF THE SYSTEM IN RESPONSE TO ‘‘LOAD CHANGES’’

It is standard procedure to respond to load variations in this context to guarantee the effective use of the newly implemented VSG control technology for the system. To assess the device's performance, an extra 1 kW load was abruptly introduced at the 0.5 s mark, as shown on the time (S) axis in Figure 10.16 (i). Figure 10.16 (i) illustrates the successful attainment of a clean reaction for energetic power. The controller's efficacy is seen in Figure 10.16 (ii), which depicts the load output responds to current variations in the load.

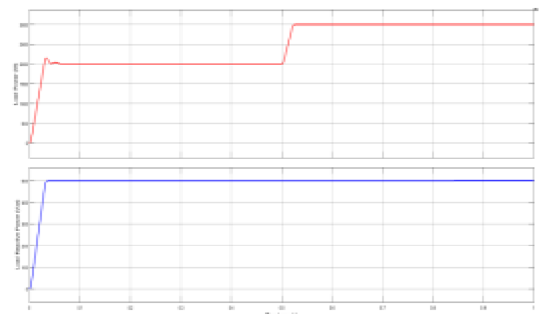

(i)

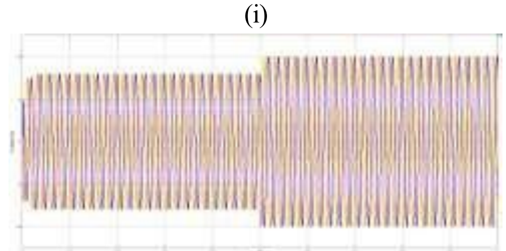

(ii)

FIGURE 10.16 Response to output load changes: (i) active and reactive power; (ii) output current

FUZZY RESULTS

An ASCII text FIS file representing a fuzzy system is saved to disc with the file extension .fis. This text file may be readily modified and interpreted. Your fuzzy system will transform into a MATLAB structure for the FIS system when saving it to the MATLAB workspace. You may provide the name of the variable that will fulfil this function. The system denoted by FIS files and structures is identical to the same system.

A. SCENARIO A: DIFFERENT IRRADIANCE VALUES

The Fig.10.17 shows the MATLAB/SIMULINK circuit diagram of the system in Scenario A and the Fig.10.18 shows the irradiation applied to the PV.

The curve, as shown in the figure, contains various irradiations with a maximum value of 1000 $W\backslash m^2$. The PV voltage and first stage voltage followed the change in radiation, as shown in Fig.10.19 (i) and Fig.10.19 (ii), respectively. At the first stage, the PV rise to 160 V and boosted voltage to 425 V. This is caused by the nature of the MPPT method in PV, and it provided details for the control behavior. The current results of the PV array and boost converter output are given in Fig.10.20 (i) and Fig.10.20 (ii), respectively. The PV current is approximately 47 A, while the boost converter current decreases to 10.5 A. This decrease depends on the design of the boost converter. Fig.10.21 shows the results of the inverter voltage and current for the output load. The inverter side is connected with the load and the output power waveforms shown in Fig.10.22.

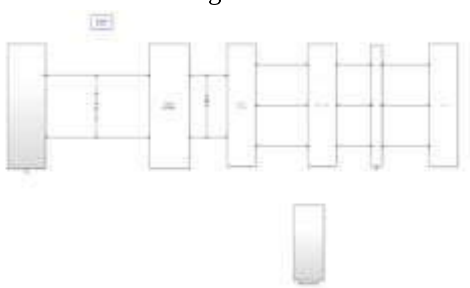

FIGURE 10.17 MATLAB/SIMULINK circuit diagram of the system in Scenario A

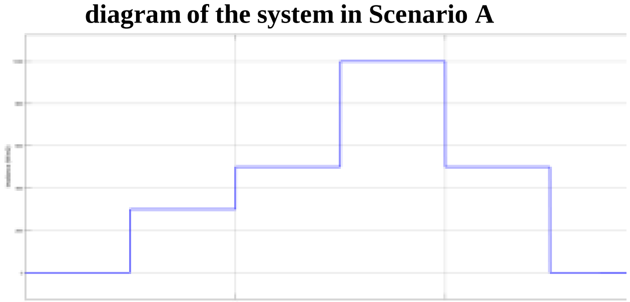

FIGURE 10.18 The irradiation scheme

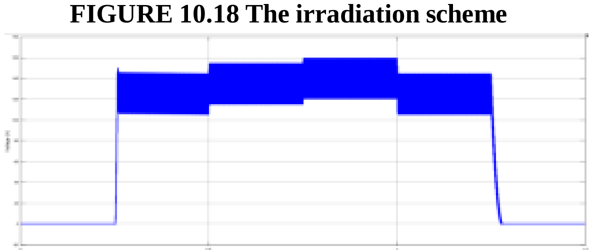

FIGURE 10.19 (i) PV voltage

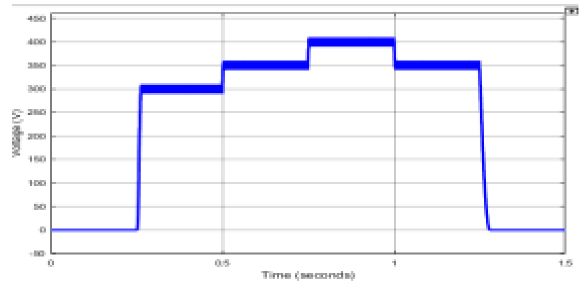

FIGURE 10.19 (ii) boost converter voltage

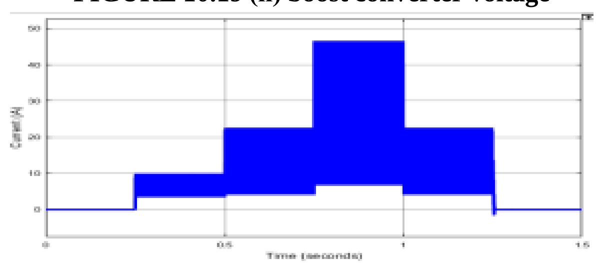

FIGURE 10.20 Current waveforms: (i) PV current

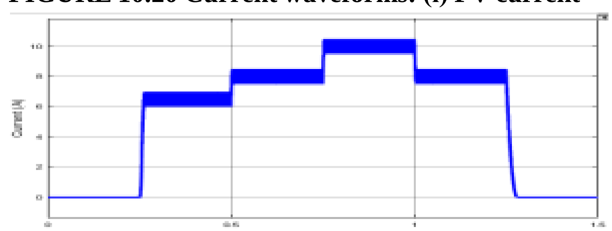

FIGURE 10.20 (ii) boost converter output current

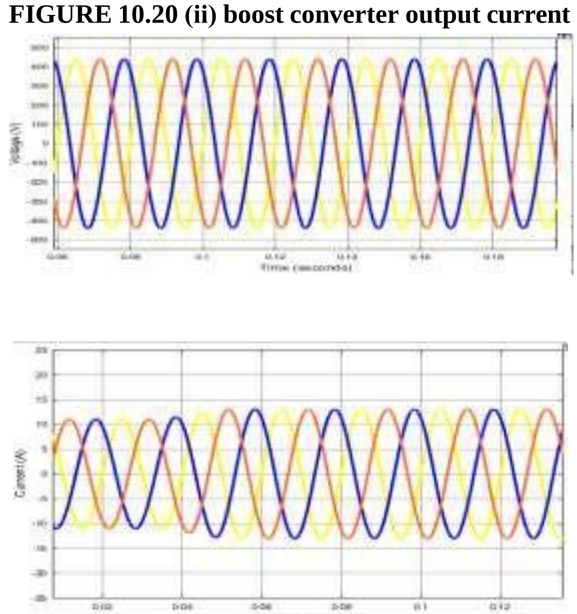

FIGURE 10.21 The output load: (i) voltage (ii) current

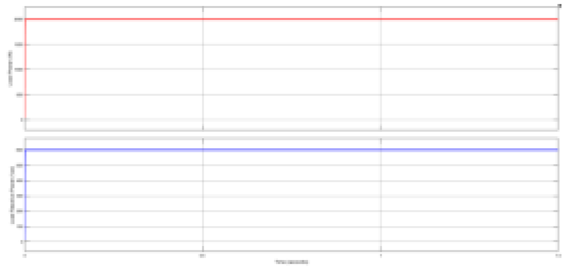

FIGURE 10.22 The load active and reactive power

B. SCENARIO B: IRRADIANCE CURVE VALUES

The Fig.10.23 shows the MATLAB/SIMULINK circuit diagram of the system in Scenario B and the Fig.11.24 shows the irradiation applied to the PV.

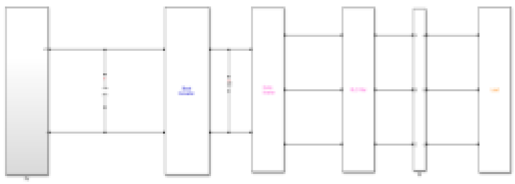

FIGURE 10.23 MATLAB/SIMULINK circuit diagram of the system in Scenario B

The curve also contains various values, as seen in the diagram Fig.10.24. The voltage response to the new irradiation curve change was plotted for PV voltage and output voltage of the DC-DC stage, as shown in Fig.10.25. In this paper, the VSG control method was used, as it provides a higher efficiency rate. The advantages of this control method are used for the inverter to behave as a synchronous generator, used for operating inverters in parallel, and for the stability of a weak power grid or islanding mode [Fig.10.26-10.28]. Fig.10.27 shows the PV array and boost converter current. The inverter side relates to the load and the output power waveforms shown Fig.10.28.

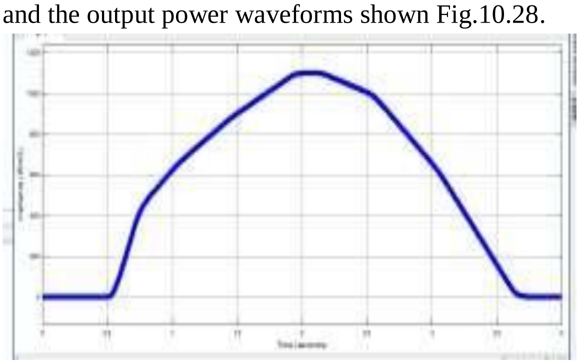

FIGURE 10.24 The irradiation scheme

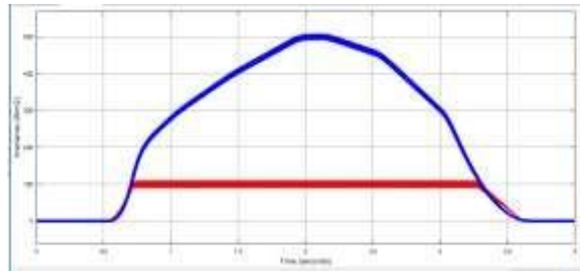

FIGURE 10.25 The PV and boost converter voltage

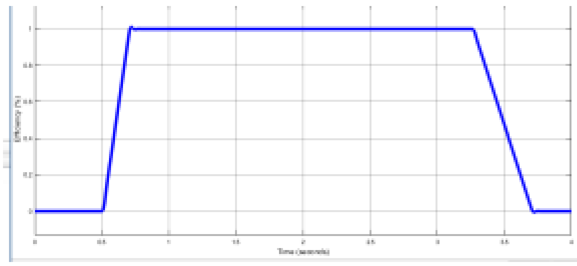

FIGURE 10.26 MPPT Eficiency

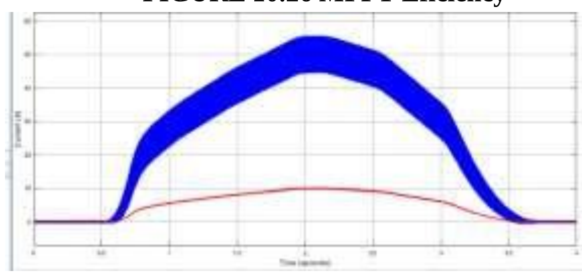

FIGURE 10.27 The PV and boost converter current

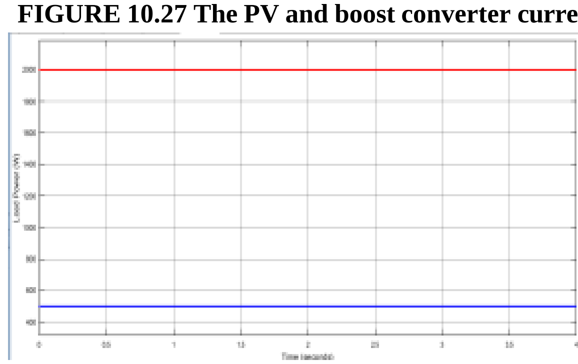

FIGURE 10.28 The load active and reactive power

C. SCENARIO C: BATTERY CHARGE AND DISCHARGE

The Fig.10.29 shows the MATLAB/SIMULINK circuit diagram of the system in Scenario B in charging mode. The arrangement as shown in figure.

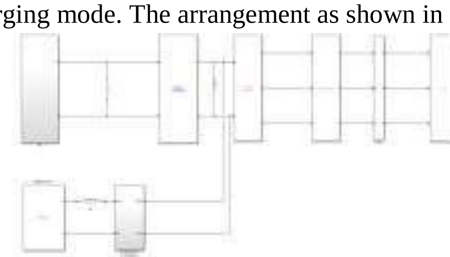

FIGURE 10.29 MATLAB/SIMULINK circuit diagram of the system in Scenario C (CHARGE MODE)

In the two cases of charging and discharging, a battery bidirectional converter is used. The voltage source ‘‘boost converter output’’ enabled the battery to charge with the load in the two cases of charging and discharging, a battery bidirectional converter is used. The voltage source ‘‘boost converter output’’ enabled the battery to charge with the load voltage is charged with a value of 225 volts, as presented in Fig.10.30 (ii) and Fig.10.30 (iv). Fig.10.30 (iii) presents the battery reference current IB on this mode selected as −20 A, and the battery charging current is -8 A.

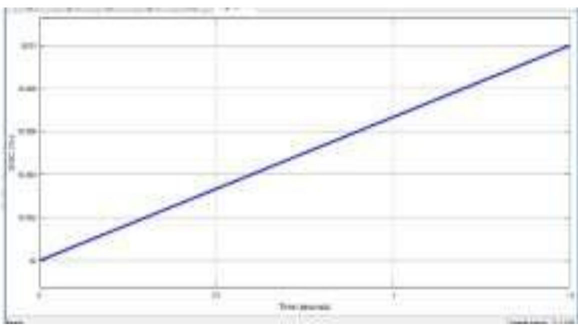

(i)

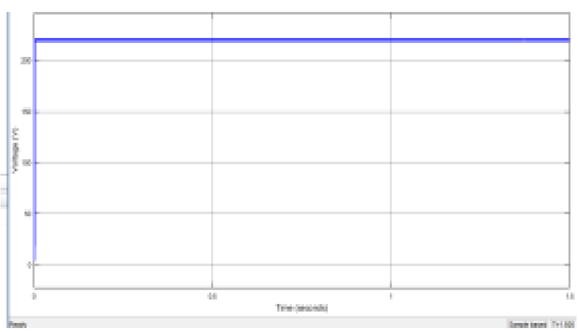

(ii)

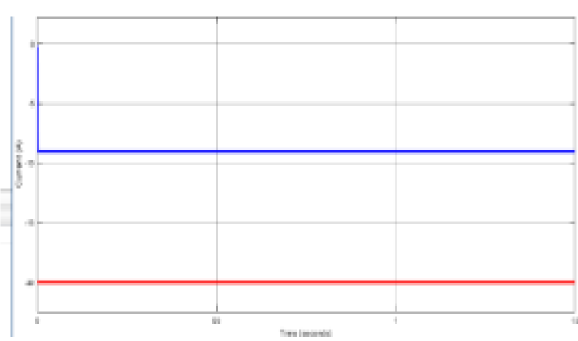

(iii)

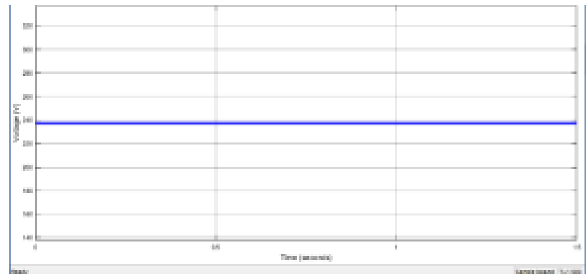

(iv)

FIGURE 10.30 Battery charge mode: (i) the state of charge; (ii) load voltage; (iii) reference and battery current; (iv) battery voltage

In the discharging mode, the source voltage is disabled, and the battery supplies the load. Fig.10.32 shows the discharge operation. The reference current is 20 A, and the battery is discharged with 238 V and 21 A. The battery is connected in scenarios A and B. The battery status results at scenarios A and B have the same results as in scenario C.

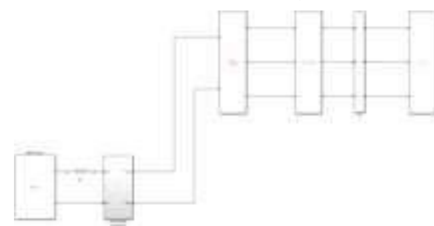

FIGURE 10.31 MATLAB/SIMULINK circuit diagram of the system in Scenario C (DISCHARGE MODE)

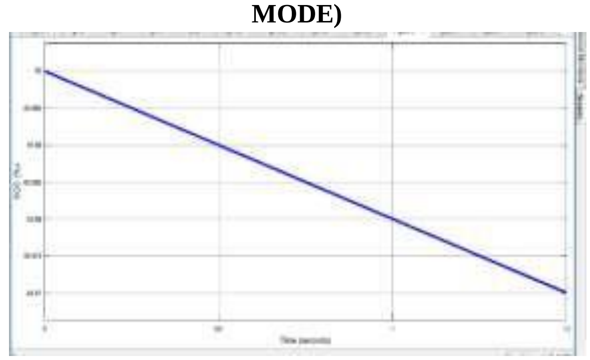

(i)

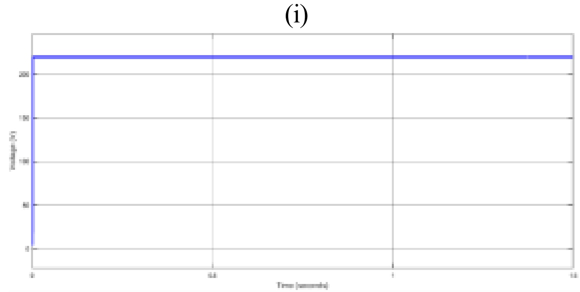

(ii)

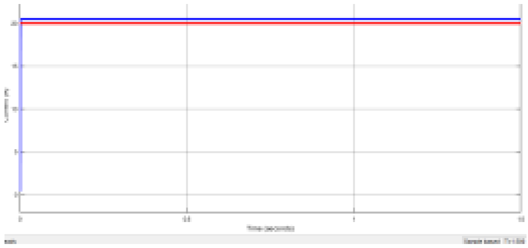

(iii)

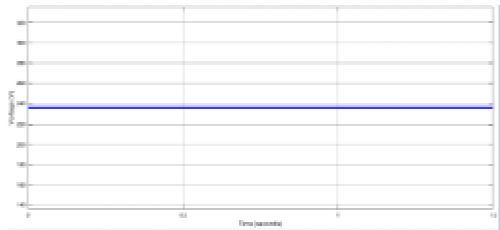

(iv)

FIGURE 10.32 Battery discharge mode: (i) the state of charge; (ii) load voltage; (iii) reference and battery current; (iv) battery voltage

D. SCENARIO D: THE BEHAVIOR OF THE SYSTEM IN RESPONSE TO ''LOAD CHANGES''

This scenario mainly discusses the response to load changes to verify the VSG control technology that has been successfully deployed to be applied effectively for this system. If the time (S) axis in Fig.10.33 (i) is observed, it is noted that at the 0.5 s mark, another load of 1 kW was added spontaneously and suddenly to evaluate the system performance. As seen, a smooth response has been achieved for active power, as shown in Fig.10.33 (i). Load output current responses under the load changes are depicted in Fig.10.33 (ii), which proves the effectiveness of the controller.

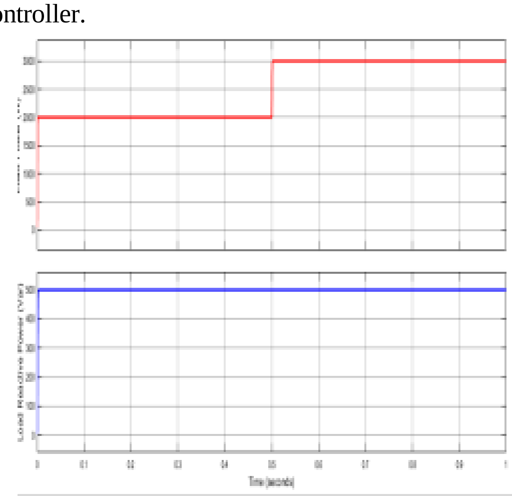

(i)

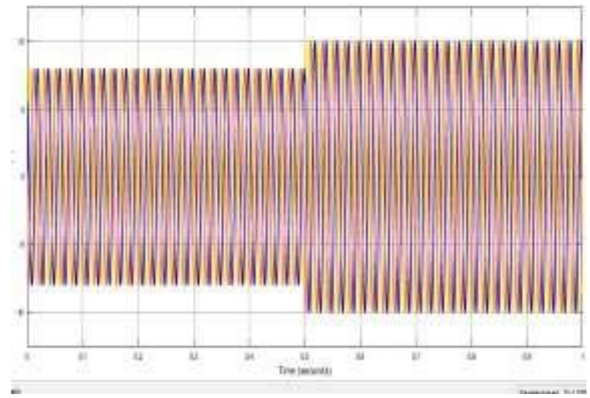

(ii)

FIGURE 10.33 Response to output load changes: (i) active and reactive power; (ii) output current

6. CONCLUSION

According to the item, a battery unit may be used with degree converter PV structures. The MPPT and VSG algorithms are used in the optimum management approach. Additionally, a bidirectional converter control is provided. The mixed manager was able to function well under a variety of irradiation settings because to the quick and responsive control capabilities of the proposed technique. The bidirectional battery approach demonstrates how managing battery modes offers additional control capabilities that have a big influence on the device as a whole and the integrated performance assessments.

REFERENCES

[1] P. S. Shenoy, K. A. Kim, B. B. Johnson, and P. T. Krein, ''Differential power processing for increased energy production and reliability of photovoltaic systems,'' IEEE Trans. Power Electron., vol. 28, no. 6, pp. 2968–2979, Jun. 2013, doi: 10.1109/TPEL.2012. 2211082.

[2] X. Lu, K. Sun, J. M. Guerrero, J. C. Vasquez, and L. Huang, ''State-of charge balance using adaptive droop control for distributed energy storage systems in DC microgrid applications,'' IEEE Trans. Ind. Electron., vol. 61, no. 6, pp. 2804–2815, Jun. 2014, doi: 10.1109/TIE.2013.2279374.

[3] M. Sechilariu, B. Wang, and F. Locment, ''Building integrated photo voltaic system with energy storage and smart grid communication,'' IEEE Trans. Ind. Electron., vol. 60, no. 4, pp. 1607–1618, Apr. 2013, doi: 10.1109/TIE.2012.2222852.

[4] Z. Liang, R. Guo, J. Li, and A. Q. Huang, ''A high-efficiency PV moduleintegrated DC/DC converter for PV energy harvest in FREEDM systems,'' IEEE Trans. Power Electron., vol. 26, no. 3, pp. 897–909, Mar. 2011, doi: 10.1109/TPEL.2011.2107581.

[5] M. Shayestegan, ''Overview of grid-connected two-stage transformer less inverter design,'' J. Mod. Power Syst. Clean Energy, vol. 6, no. 4, pp. 642–655, Jan. 2018, doi: 10.1007/s40565-017-0367-z.

[6] S. Wei, F. He, L. Yuan, Z. Zhao, T. Lu, and J. Ma, ''Design and implementation of high efficient two-stage three-phase/level isolated PV converter,'' in Proc. 18th Int. Conf. Electr. Mach. Syst. (ICEMS), Pattaya, Thailand, Oct. 2015, pp. 1649–1654.

[7] A. Sangwongwanich and F. Blaabjerg, ''Mitigation of interharmonics in PV systems with maximum power point tracking modification,'' IEEE Trans. Power Electron., vol. 34, no. 9, pp. 8279–8282, Sep. 2019, doi: 10.1109/TPEL.2019.2902880.

[8] R. Boukenoui, M. Ghanes, J.-P. Barbot, R. Bradai, A. Mellit, and H. Salhi, ''Experimental assessment of maximum power point tracking methods for photovoltaic systems,'' Energy, vol. 132, pp. 324–340, Aug. 2017, doi: 10.1016/j.energy.2017.05.087.

[9] N. A. Ninad and L. A. C. Lopes, ''Operation of single-phase gridconnected inverters with large DC bus voltage ripple,'' in Proc. IEEE Canada Electr. Power Conf., Montreal, QC, Canada, Oct. 2007, pp. 172–176, doi: 10.1109/EPC.2007.4520325.

[10] S. B. Kjaer, J. K. Pedersen, and F. Blaabjerg, ''A review of single phase grid-connected inverters for photovoltaic modules,'' IEEE Trans. Ind. Appl., vol. 41, no. 5, pp. 1292–1306, Sep. 2005, doi: 10.1109/TIA.2005.853371.

[11] R. Wai and W. Wang, ''Grid-connected photovoltaic generation system,'' IEEE Trans. Circuits Syst., vol. 55, no. 3, pp. 953–963, Apr. 2008, doi: 10.1109/TCSI.2008.919744.

[12] D. Debnath and K. Chatterjee, ''Transformer coupled multi-input two stage standalone solar photovoltaic scheme for rural areas,'' in Proc. 39th Annu. Conf. IEEE Ind. Electron. Soc. (IECON), Vienna, Austria, Nov. 2013, pp. 7028–7033, doi: 10.1109/IECON.2013.6700298.

[13] T.-F. Wu, ''Power loss comparison of Single- and two-stage grid-connected photovoltaic systems,'' J. Electr. Electron. Eng., vol. 26, no. 2, pp. 11–19, Jun. 2014, doi: 10.1109/TEC.2011.2123897.

[14] N. H. Selman and J. R. Mahmood, ''Design and simulation of two stages single phase PV inverter operating in standalone mode without batteries,'' Int. J. Eng. Trends Technol., vol. 37, no. 2, pp. 102–109, Jul. 2016, doi: 10.14445/22315381/IJETT-V37P217.

[15] Y. Amara, R. Boukenoui, R. Bradai, and H. Salhi, ''Design and control of two-stage standalone photovoltaic generation system,'' in Proc. Int. Conf. Commun. Electr. Eng. (ICCEE), El Oued, Algeria, Dec. 2018, pp. 1–5, doi: 10.1109/CCEE.2018.8634511

[16] N. Guler and E. Irmak, ''MPPT based model predictive control of grid connected inverter for PV systems,'' in Proc. 8th Int. Conf. Renew. Energy Res. Appl. (ICRERA), Brasov, Romania, Nov. 2019, pp. 982–986.

[17] J. Alipoor, Y. Miura, and T. Ise, ''Distributed generation grid integration using virtual synchronous generator with adoptive virtual inertia,'' in Proc. IEEE Energy Convers. Congr. Expo. (ECCE), Denver, CO, USA, Sep. 2013, pp. 4546–4552.

[18] J. Alipoor, Y. Miura, and T. Ise, ''Power system stabilization using virtual synchronous generator with alternating moment of inertia,'' IEEE J. Emerg. Sel. Topics Power Electron., vol. 3, no. 2, pp. 451–458, Jun. 2015, doi: 10.1109/JESTPE.2014.2362530.

[19] K. Sakimoto, Y. Miura, and T. Ise, ''Stabilization of a power system with a distributed generator by a virtual synchronous generator function,'' in Proc. 8th Int. Conf. Power Electron. (ECCE Asia), Jeju, South Korea, May/Jun. 2011, pp. 1498–1505.

[20] S. Rubino, A. Mazza, G. Chicco, and M. Pastorelli, ''Advanced control of inverter-interfaced generation behaving as a virtual synchronous generator,'' in Proc. IEEE Eindhoven PowerTech, Eindhoven, The Netherlands, Jun./Jul. 2015, pp. 1–6.